

LabVIEW Based Simulation of Static VAR Compensator for Transient Stability Enhancement in Electric Power Systems

¹Lini Mathew and ²S. Chatterji

*¹Associate Professor, ²Professor and Head,
Electrical Engineering Department,
National Institute of Technical Teachers Training and Research,
Sector 26, Chandigarh, 160019, India
E-mail: lenimathew@yahoo.com, chatterjis@yahoo.com*

Abstract

Power system engineers are currently facing challenges to increase the power transfer capabilities of existing transmission system. Flexible AC Transmission System (FACTS) controllers are capable of power flow balancing and thereby implementing the most efficient and effective use of the existing power system network. FACTS controllers by virtue of their fast response can improve the stability of an electrical power system by way of helping critically disturbed generators to give away the excess energy gained through acceleration due to a fault or disturbance. Static VAR Compensator (SVC) is a key shunt connected FACTS controller and is widely recognized. It serves as an effective means to enhance power system stability. In the present work the authors have made an attempt to generate a mathematical model of SVC by simulating the device in terms of transfer function model. The proposed model of the SVC controller has been tested by incorporating the same in a simple single-machine infinite-bus (SMIB) system as well as in a multi-machine power system.

LabVIEW software has been employed for the simulation purpose. LabVIEW is a new research tool which is capable of representing dynamic systems in block diagram form, along with the provision of simulation of the system behaviour in totality. This simulation technique also reduces the system complexity from a developer's standpoint, and thus allows the researchers to concentrate on the application details. Such facilities are not available in the traditional means of measurement techniques and tools. Simulation results are encouraging and indicate that the proposed simulation model is very close to the physical simulation.

Keywords: FACTS, Multi-machine power system, SMIB system, Static VAR Compensator, Transient stability.

Introduction

Transmission interconnections are done for economic reasons, taking advantage of diversity of loads, availability of sources and fuel prices, in order to supply electricity to the loads at minimum cost with a stipulated degree of reliability. An effective electric grid, is a fully interconnected system where power stations, transmission lines and distribution feeders are all inflexibly tied up by the synchronous constraints. With the increased loading of transmission lines, the problem of transient stability due to a major fault can cause hindrances which may become a transmission power limiting factor.

The power system thus, must call for flexibility so that it can adapt to momentary changes in system conditions. This need of the power system has given birth to the nomenclature called Flexible AC Transmission System (FACTS). The idea of FACTS was introduced way back in 1980s.

Power System Stability (PSS)

Power systems are exposed to various dynamic disturbances, which may cause a sudden imbalance between active and reactive powers of the system and consequently pose a problem in certain machines. This disturbance depending on its severity may result into de-synchronization of the machine from the power system. In spite of such erratic behaviour, the power system possesses the capability to recover from such an undesired situation. This capability of the system to recover from disturbances and regain the steady-state synchronism under stipulated contingency conditions is characterized as *power system stability*. The aspect of stability is influenced by the dynamics of generator rotor-angles. A power system is transiently stable, if following a large disturbance, the system angle spread starts to increase but reaches a peak and then starts declining, and reaches a steady state operating condition [1,2]. Transient stability is the capability of the power system to maintain synchronism under the condition of a severe and fast disturbance in the system. The maximum amount of steady state power that the system after being subjected to a fault, can transmit for specified operating conditions without losing synchronism is known as the *transient stability limit* of the system.

The use of FACTS controllers in power transmission system not only enhances the system stability but also brings in flexibility to the power system.

Facts Controllers

FACTS as per IEEE is defined as “ac transmission systems incorporating power electronics-based and other static controllers for enhancing controllability and increasing power transfer capability”. Similarly, a FACTS Controller may be defined as “a power-electronics based control system along with some other static equipment,

capable of implementing control of one or more ac transmission system parameters.”

FACTS controllers refer to devices that enable flexible electrical power system operation, in the way of controlled active and reactive power flow redirection in transmission paths, by means of flexible and rapid control over the ac transmission parameters [3].

FACTS technology opens up new opportunities for controlling and enhancing the useable capacity of present, as well as new upgraded lines. These opportunities arise through the capabilities of FACTS controllers to control the inter-related parameters including series impedance, shunt impedance, current, voltage, phase-angle and the damping of oscillations at various frequencies below the rated frequency, that govern the operation of transmission system. In other words it can be said that FACTS controllers can facilitate the power system control, by enhancing the power transfer capacity, decreasing the line losses and generation costs, and thus improve the stability and security of the power system [4].

Static VAR Compensator (SVC)

A static VAR compensator (SVC) is a shunt connected static generator or absorber of reactive power in which the output is varied to maintain or control specific parameters of the electrical power system. VAR compensation is used for voltage regulation either at the mid-point or at some intermediate-point in order to segment the transmission line and at the end of the line in order to prevent voltage instability, and also for dynamic voltage control to increase transient stability and damp power oscillations.

SVC functions as a variable reactance capable of operating in both inductive and capacitive regions as per requirement on a cycle by cycle basis to provide compensation at the point of connection to the power system. Voltage regulation is the operational objective of the SVC. Transient response of SVC controlled systems thus impacts much on the overall power system performance and hence inappropriate settings may lead to voltage instability.

SVC may also be taken as an automated impedance matching device. If the power system's reactive load is capacitive in nature, the SVC will use reactors to supply VARs to the system, bringing the system closer to unity power factor and thus lowering the system voltage. A similar process is carried out with an inductive load condition, providing a power factor closer to unity and, consequently, increasing the system voltage [5]. SVCs are cheaper, faster, and more reliable as compared to dynamic compensation schemes such as synchronous compensators/condensers, popularly known as STATCOM.

Single-Machine Infinite-Bus (SMIB) System Modeling

In the present work, simulation of SVC controller incorporated on a Single-Machine Infinite-Bus (SMIB) System using LabVIEW 8.2 version has been carried out. Performance of such a system has been investigated by analyzing the system. This has been achieved by varying the system parameters. The model proposed in the present

work finds sufficient scope for transient stability enhancement. Fig.1 shows a single-line diagram of SMIB system incorporated with SVC Controller.

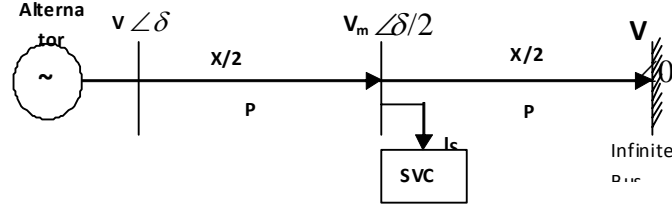


Figure 1: SVC connected at the mid-point of a SMIB power system.

The system equations as discussed in [6] are given by:

$$\frac{d\delta}{dt} = \omega_B(S_m - S_{m0}) \quad (1)$$

$$\frac{dS_m}{dt} = \frac{1}{2H}[-D(S_m - S_{m0}) + T_m - T_e] \quad (2)$$

$$\frac{dE'_q}{dt} = \frac{1}{T'_{do}}[-E'_q + (x_d - x'_d)i_d + E_{fd}] \quad (3)$$

$$\frac{dE'_d}{dt} = \frac{1}{T'_{qo}}[-E'_d + (x_q - x'_q)i_q] \quad (4)$$

where δ is the rotor angle of synchronous generator in radians, ω_B is the rotor speed deviation in rad/sec, S_m is the generator slip in p.u., S_{m0} is the initial operating slip in p.u., H is the inertia constant, D is the damping coefficient, T_m is the mechanical power input in p.u., T_e is the electrical power output in p.u., E_{fd} is the system excitation voltage in p.u., T'_{do} is the open circuit d-axis time constant in sec., T'_{qo} is the open circuit q-axis time constant in sec., x_d is the d-axis synchronous reactance in p.u., x'_d is the d-axis transient reactance in p.u., x_q is the q-axis synchronous reactance in p.u., x'_q is the q-axis transient reactance in p.u.,

The electrical torque T_e is expressed in terms of variables E'_d, E'_q, i_d, i_q as:

$$T_e = E'_d i_d + E'_q i_q + (x'_d - x'_q) i_d i_q \quad (5)$$

For a lossless network, the stator algebraic equations and the network equations can be expressed as:

$$E'_q + x'_d i_d = V_q \quad (6)$$

$$E'_d - x'_q i_q = V_d \quad (7)$$

$$V_q = -x_e i_d + E_b \cos \delta \quad (8)$$

$$V_d = x_e i_q - E_b \sin \delta \quad (9)$$

Solving the above equations, the variables i_d and i_q can be obtained as:

$$i_d = \frac{E_b \cos \delta - E'_q}{x_e + x'_d} \tag{10}$$

$$i_q = \frac{E_b \sin \delta + E'_q}{x_e + x'_q} \tag{11}$$

where E_b is the infinite bus voltage in p.u., V_t is the generator terminal voltage in p.u., f is the nominal frequency = 50 Hz.

Multi-Machine (MM) System Modeling

The popular Western System Coordinated Council (WSCC) 3-machines 9-bus practical power system with loads assumed to be represented by constant impedance model has been considered as the second test case as a multi-machine power system. Fig.2 shows the WSCC 3-machines 9-bus system.

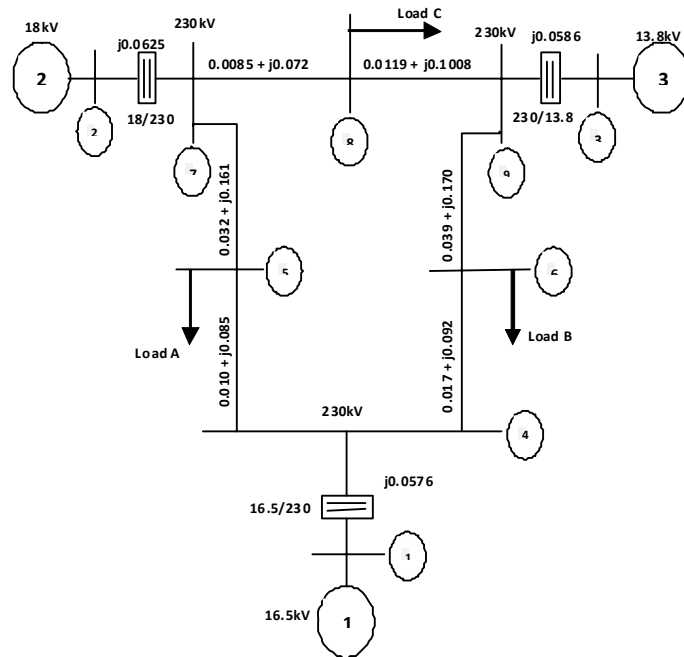


Figure 2: WSCC 3-Machines 9-Bus System.

WSCC system is widely used and found very frequently in the relevant literature [7,8,9]. The base MVA of the system is 100, and system frequency is 60 Hz. The disturbance, for the power system under study, initiating the transient has been considered as a three-phase fault occurring near bus number 7 at the end of the line 5-7. This initializes that the SVC needs to be located at bus number 5 because VAR compensation is to be used for voltage regulation either at the mid-point or at some

intermediate-point in order to segment the transmission line and at the end of the line for preventing voltage instability, and also for obtaining dynamic voltage control to increase transient stability by damping power swings and oscillations.

The Y matrix for each network condition (pre-fault and during-fault) is formed. The Y matrix for the reduced network is obtained by eliminating all nodes except for the internal generator nodes. The reduction can be achieved by matrix operation with the fact in mind that all the nodes have zero injection currents, except, for the internal generator nodes.

For a power system comprising n generators, the nodal equation can be written as:

$$\begin{bmatrix} I_n \\ 0 \end{bmatrix} = \begin{bmatrix} Y_{nn} & Y_{nr} \\ Y_{rn} & Y_{rr} \end{bmatrix} \begin{bmatrix} V_n \\ V_r \end{bmatrix} \quad (12)$$

where, the scripts n and r are used to denote the numbers of generator nodes and terminal nodes respectively. Expanding eqn (12), we get:

$$\begin{aligned} I_n &= Y_{nn} V_n + Y_{nr} V_r \\ 0 &= Y_{rn} V_n + Y_{rr} V_r \end{aligned}$$

V_r can be eliminated to find

$$I_n = (Y_{nn} - Y_{nr} Y_{rr}^{-1} Y_{rn}) V_n \quad (13)$$

Thus, the desired reduced matrix can be written as:

$$Y_r = (Y_{nn} - Y_{nr} Y_{rr}^{-1} Y_{rn}) \quad (14)$$

It has $(n \times n)$ dimensions where n denotes the number of generators. The network reduction illustrated by eqns (12) – (14) is a convenient analytical technique that can be used only when the loads are treated as constant impedances [10].

The resultant reduced Y matrices of the system before, and during fault conditions are worked out and are given as Y_{Rpf} and Y_{Rdf} respectively.

The reduced Y matrix for the network in the pre-fault condition is given by:

$$Y_{Rpf} = \begin{bmatrix} 0.8455 - 2.9883i & 0.2871 + 1.5129i & 0.2096 + 1.2256i \\ 0.2871 + 1.5129i & 0.4200 - 2.7239i & 0.2133 + 1.0879i \\ 0.2096 + 1.2256i & 0.2133 + 1.0879i & 0.2770 - 2.3681i \end{bmatrix} \quad (15)$$

Similarly, reduced Y matrix for the network during-fault condition is given by:

$$Y_{Rdf} = \begin{bmatrix} 0.6568 - 3.8160i & 0 & 0.0701 + 0.6306i \\ 0 & 0 - 5.4855i & 0 \\ 0.0701 + 0.6306i & 0 & 0.1740 - 2.7959i \end{bmatrix} \quad (16)$$

The power flowing into the network at node i , which is same as the electrical power output of machine i , is given by:

$$P_{ei} = E_i^2 G_{ii} + \sum_{\substack{j=1 \\ j \neq i}}^3 E_i E_j Y_{ij} \cos(\theta_{ij} - \delta_i + \delta_j) \quad (17)$$

where, $i = 1, 2$ and 3

$$\bar{Y}_{ij} = Y_{ij} \angle \theta_{ij} = G_{ij} + jB_{ij}$$

is the negative of the transfer admittance between nodes i and j

$$\bar{Y}_{ii} = Y_{ii} \angle \theta_{ii} = G_{ii} + jB_{ii}$$

is the driving point admittance of node i

The equations of motion are then given by:

$$\frac{2H_i}{\omega_R} \frac{d\omega_i}{dt} + D_i \omega_i = P_{mi} - [E_i^2 G_{ii} + \sum_{\substack{j=1 \\ j \neq i}}^3 E_i E_j Y_{ij} \cos(\theta_{ij} - \delta_i + \delta_j)] \quad (18)$$

and,

$$\frac{d\delta_i}{dt} = \omega_i - \omega_r \quad (19)$$

Prior to the disturbance ($t = 0$), $P_{mi0} = P_{ei0}$

Thereby,

$$P_{mi0} = E_i^2 G_{ii0} + \sum_{\substack{j=1 \\ j \neq i}}^3 E_i E_j Y_{ij0} \cos(\theta_{ij0} - \delta_{i0} + \delta_{j0}) \quad (20)$$

The subscript 0 has been used to indicate the pre-transient conditions.

As the network parameters change due to switching during the fault, the corresponding values will be incorporated in the equations (17) and (18).

LabVIEW Based Models of SMIB and MM Systems without Incorporating SVC in the Power System

LabVIEW is a very powerful and flexible tool. It is basically a software package having provision of environment for graphical development. LabVIEW enables simulation of instrumentation schemes and their analysis. It can create flexible and scalable design, control, and test applications [11]. LabVIEW has features regarding built-in virtual instrument modules and can thus provide a graphical environment for simulation. It can produce a visual representation of the system. The software has a high potential for the analysis of system performance and can be used in simulation techniques effectively.

Data for the SMIB system under study are as under:

$x_d = 1.7572$, $x'_d = 0.4245$, $T'_{do} = 4$, $x_q = 1.5845$, $x'_q = 1.04$, $T'_{qo} = 1.22$, $S_{mo} = 0$, $D = 100$, $H = 50$, $T_m = 1$, $E_b = 0.089$, $X_T = 0.1364$, $X_L = 0.8125$, $X_{TH} = 0.13636$ [7] ,

where, X_T represents the reactance of the transformer per circuit, X_L represents the reactance of transmission line per circuit and X_{TH} represents the Thevenin's impedance of the receiving end system.

The LabVIEW based model of the SMIB System with the given data without incorporating SVC controller in the power system is shown in Fig.3.

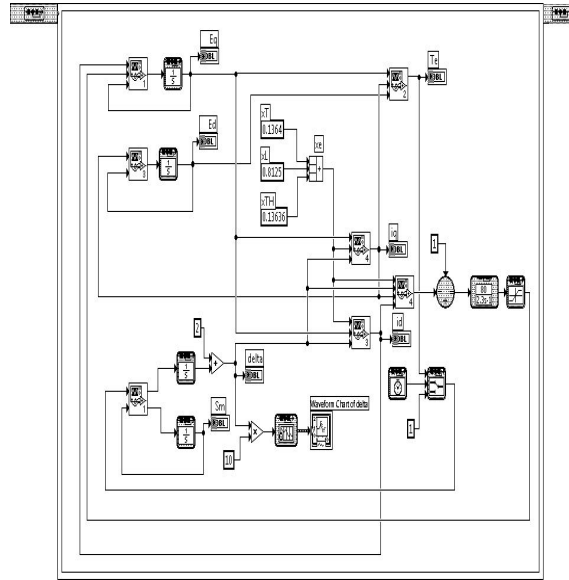


Figure 3: LabVIEW Based Model of SMIB System without incorporating SVC in the power system.

The LabVIEW based model of the 3-machine 9-bus system with the given data without incorporating SVC controller in the power system is shown in Fig.4.

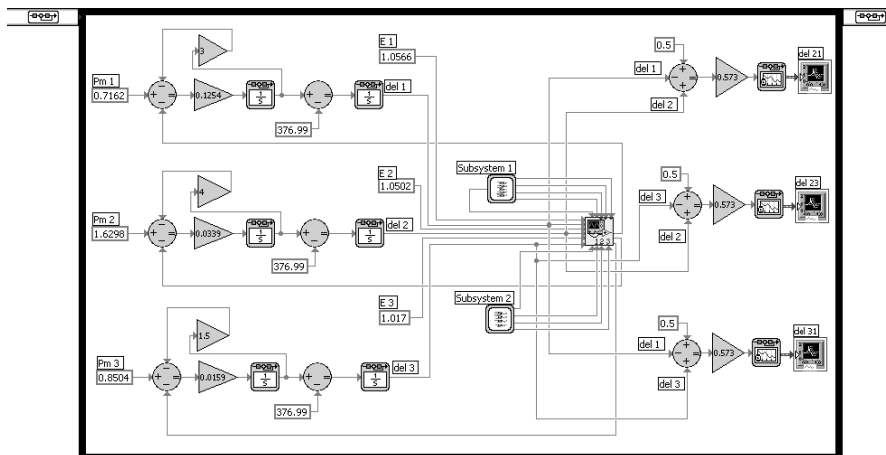


Figure 4: LabVIEW Based Model of WSCC 3-Machines 9-Bus System without incorporating SVC in the Power System.

Transfer Function Model of the SVC Controller

The transfer function model of the SVC controller is shown in Fig.5 [12,13].

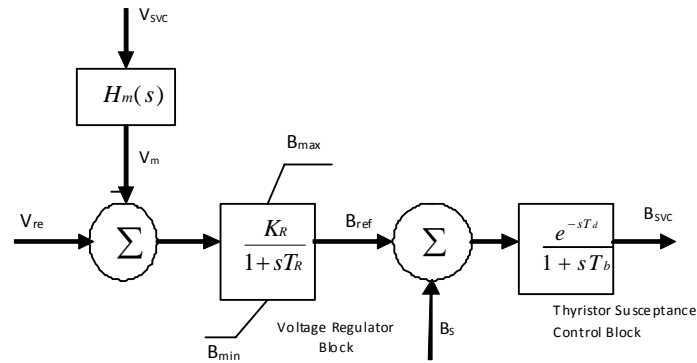


Figure 5: Transfer Function Model of the SVC Controller.

Input to the SVC controller ($V_{ref} - V_{SVC}$) is fed to the voltage regulator block of SVC. Output of voltage regulator block B_{ref} is fed to the thyristor susceptance control block whose output is B_{SVC} . Output of the SVC controller B_{SVC} , is the susceptance of the SVC controller. V_{SVC} is the SVC voltage, V_m is the voltage output of the measuring model, B_{ref} is the reference value of SVC susceptance.

Transfer function of the measuring model $H_m(s)$ is given by:

$$H_m(s) = \frac{1}{1 + sT_m} \tag{21}$$

where, T_m is the time constant associated with the measuring model and is typically equal to 2 to 3 ms.

The thyristor susceptance control block is represented by:

$$H_t(s) = \frac{e^{-sT_d}}{1 + sT_b} \tag{22}$$

where, T_d is the transport delay given by:

$$T_d = T/12 \tag{23}$$

where, T is the time period of the supply voltage. T_d arises due to the discrete nature of the firing pulse. T_b represents the maximum (average) delay when B_{ref} changes from maximum (B_L) to zero and is given by:

$$T_b = T/4 \tag{24}$$

The transfer function of the voltage regulator block $H_v(s)$ is given by:

$$H_v(s) = \frac{K_R}{1 + sT_R} \quad (25)$$

where K_R is the gain associated with the voltage regulator block and T_R is the time constant. Value of K_R varies typically from 20 to 100, whereas, value of T_R varies from 20 to 150ms.

B_{SVC} is used as a control signal in order to change the reactive power to be fed to the system, for altering the power flow in the line so as to bring the system back to stable conditions. Value of B_{SVC} can be changed by varying the values of damping constant D and the controller parameters K_R , T_R and T_b . This in turn will vary the power flow in the line and thus change the rotor angle, achieving the system stability conditions accordingly. Fig.6 shows the LabVIEW based model of the SVC controller. The LabVIEW (8.2 version) based Model of SMIB system incorporating the SVC controller in the power system has been developed and shown in Fig.7.

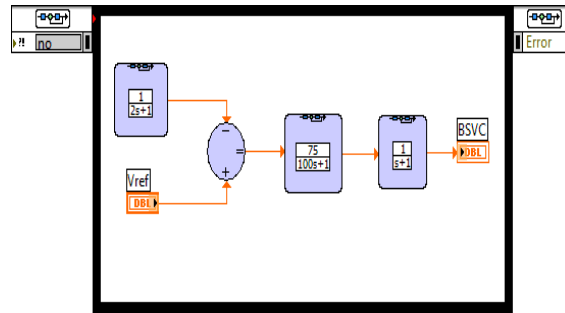


Figure 6: LabVIEW based Model of the SVC Controller.

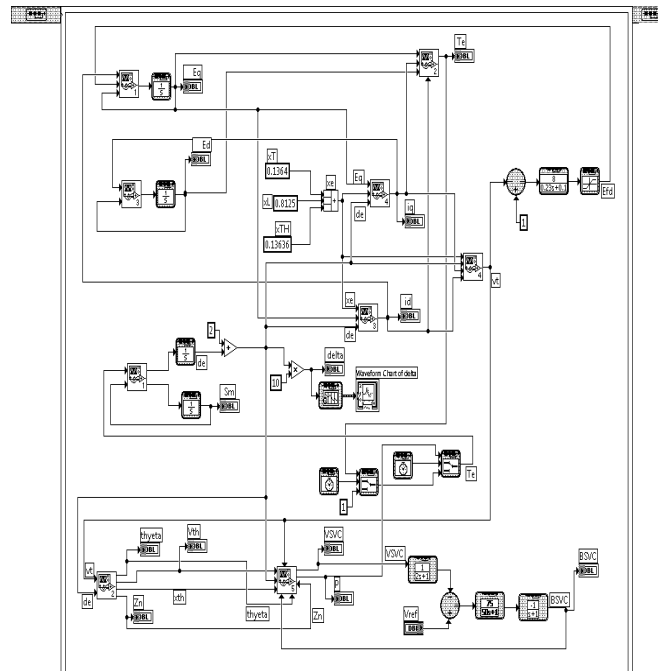


Figure 7: LabVIEW Based Model of SMIB System Incorporating SVC Controller in the Power System.

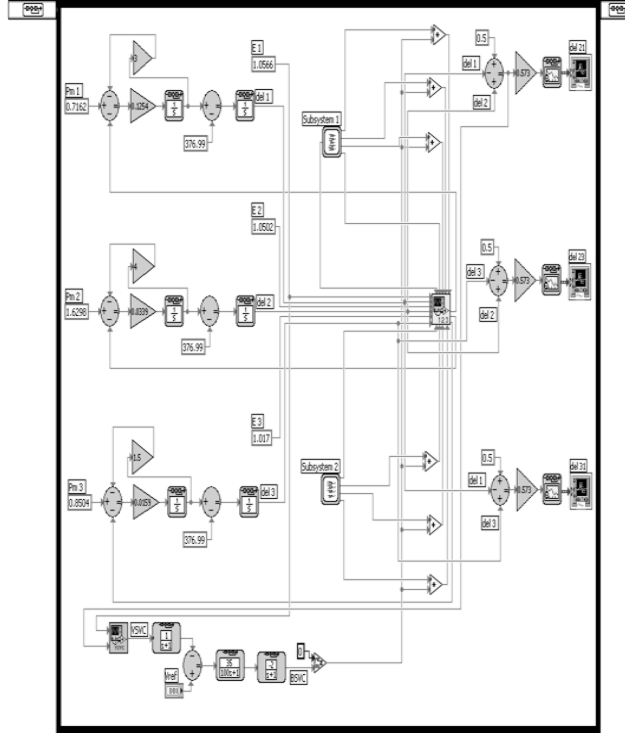


Fig 4.8 LabVIEW Model of WSCC 3-Machines 9-Bus System with SVC

Figure 8: LabVIEW Model of WSCC 3-Machines 9-Bus System Incorporating SVC Controller in the Power System.

The LabVIEW based model of the WSCC 3-machine 9-bus system incorporating the SVC controller in the power system is shown in Fig.8.

Simulation Results of the SMIB Power System Incorporated with SVC in the Power System and Discussions

The LabVIEW based simulated model of SMIB along with SVC controller incorporated in the power system has been analyzed for different conditions. The total simulation time taken is found to be equal to 20 sec. The SVC controller parameters are as under:

$$T_m = 2, K_R = 75, T_R = 100, T_d = 0.0016, T_b = 1.$$

Rotor angle (δ) variation with time for the SMIB system equipped with SVC controller has been shown in Fig.9. The curve shown in Fig.9 indicates that the system attains stability at a faster rate on reactive power compensation provided by the SVC controller incorporated in the SMIB power system. δ vs. time curve has been analyzed at various instants of time. At $t=0$, the initial value of rotor angle δ is 20^0 and

it reaches its maximum value of around 44° at $t=1.5$ sec. At this point the system tends to become unstable. The SVC controller at this moment of time, injects a particular value of reactive power into the transmission line, to bring the system back to stability.

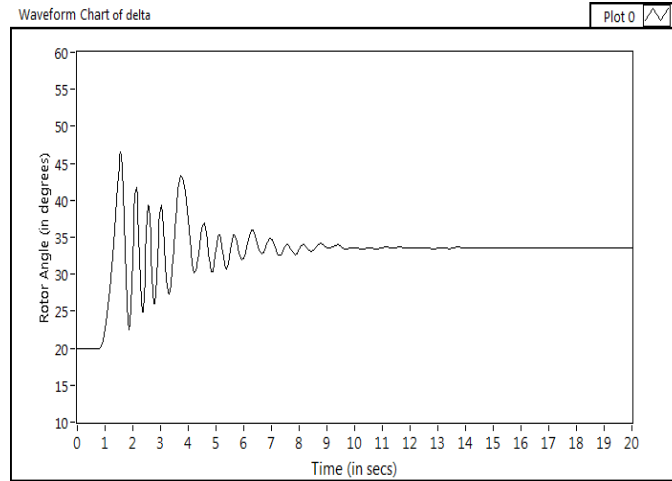


Figure 9: Variation of Rotor-angle with time for $D = 10$.

It can be observed from the curve shown in Fig.9 that as a result of reactive power injection into the transmission line, the value of rotor-angle decreases to 33.48° at $t=12$ sec. It can be inferred that during this time interval, the system attains stability. The damping constant D has been varied during the investigation process and the variation of rotor-angle δ , with time has been studied. The time taken to attain stability and the stable value of rotor-angle, for different values of damping constant D are given in Table I. Table I reveals that the system attains stability at a faster rate, when the value of damping constant is increased. This is clearly verified as the system oscillations get reduced to almost nil at higher values for damping constant. The value of the maximum overshoot of the first swing also reduces with increasing damping constant.

Table I: Time Taken to Attain Stability and Stable Value of Rotor Angle with Different Values of Damping Constant D .

Damping constant (D)	Stable value of delta (degrees)	Time Taken to Attain Stability (seconds)	Maximum Overshoot (degrees)
0	33.4118	82-83	52
1	33.3891	44-45	50
2	33.4283	33-34	49
3	33.5094	26-27	48
4	33.5358	22-23	47

5	5	0.2882	0.2867	0.288	53-54	47-48	57-58	0.408	0.4	0.32
	10	0.2885	0.2874	0.2876	49-50	45-46	49-50	0.408	0.4	0.35
	20	0.2889	0.2874	0.2880	47-48	49-50	49-50	0.415	0.4	0.35
	30	0.2896	0.2875	0.2886	46-47	49-50	49-50	0.42	0.4	0.35
	40	0.2897	0.2875	0.2887	47-48	49-50	47-48	0.425	0.4	0.335
	50	0.2898	0.2875	0.2888	45-46	46-47	45-46	0.43	0.4	0.34
10	5	0.2878	0.2875	0.2868	38-39	38-39	36-37	0.39	0.38	0.312
	10	0.2882	0.2876	0.2872	37-38	34-35	35-36	0.39	0.38	0.315
	20	0.2893	0.2878	0.2880	34-36	32-33	33-34	0.395	0.38	0.31
	30	0.2897	0.2878	0.2884	31-32	32-33	32-33	0.4	0.38	0.31
	40	0.2899	0.2878	0.2887	30-31	32-33	31-32	0.405	0.38	0.32
	50	0.2901	0.2878	0.2889	30-31	31-32	30-31	0.405	0.38	0.325
20	5	0.2871	0.2871	0.2865	20-21	23-24	22-23	0.37	0.355	0.318
	10	0.2881	0.2880	0.2869	19-20	22-23	21-22	0.368	0.355	0.31
	20	0.2893	0.2881	0.2876	18-19	21-22	20-21	0.37	0.355	0.306
	30	0.2898	0.2882	0.2881	17-18	20-21	19-20	0.37	0.355	0.306
	40	0.2901	0.2882	0.2885	16-17	18-19	19-20	0.37	0.355	0.307
	50	0.2905	0.2882	0.2888	16-17	17-18	18-19	0.375	0.355	0.31
30	5	0.288	0.2882	0.2863	16-17	17-18	16-18	0.358	0.338	0.318
	10	0.2883	0.2882	0.2866	14-15	14-15	15-16	0.356	0.338	0.31
	20	0.2888	0.2882	0.2871	13-14	13-14	14-15	0.355	0.337	0.305
	30	0.2893	0.2882	0.2876	13-14	12-13	14-15	0.354	0.337	0.304
	40	0.2896	0.2882	0.288	13-14	13-14	15-16	0.356	0.338	0.305
	50	0.2899	0.2882	0.2882	13-14	13-14	15-16	0.356	0.338	0.304
40	5	0.2878	0.2882	0.2861	17-18	16-17	16-17	0.349	0.328	0.316
	10	0.2881	0.2882	0.2864	11-12	13-14	14-15	0.345	0.328	0.308
	20	0.2886	0.2882	0.2869	10-11	11-12	13-14	0.342	0.328	0.304
	30	0.2890	0.2882	0.2873	10-11	11-12	13-14	0.343	0.328	0.303
	40	0.2893	0.2882	0.2876	10-11	11-12	13-14	0.345	0.327	0.303
	50	0.2896	0.2882	0.2879	11-12	11-12	13-14	0.345	0.327	0.304
50	5	0.287	0.2872	0.2863	16-17	13-14	16-17	0.343	0.323	0.315
	10	0.2888	0.2891	0.2868	11-12	12-13	11-12	0.338	0.321	0.308
	20	0.2894	0.2891	0.2868	10-11	11-12	10-11	0.335	0.321	0.304
	30	0.2899	0.2891	0.2873	10-11	11-12	10-11	0.335	0.32	0.302
	40	0.2904	0.289	0.2878	10-11	11-12	10-11	0.336	0.321	0.302
	50	0.2907	0.289	0.2882	10-11	11-12	10-11	0.336	0.32	0.302

When damping constants $D_2 = D_3 = 5$ kept constant and D_1 is varied from 5 to 50, the time taken to attain stability reduces by 12 seconds. Similarly when damping constants $D_2 = D_3 = 50$ kept constant and D_1 is varied from 5 to 50, the time taken to attain stability reduces only by 6 seconds. The system becomes sluggish and the oscillations reduce to zero.

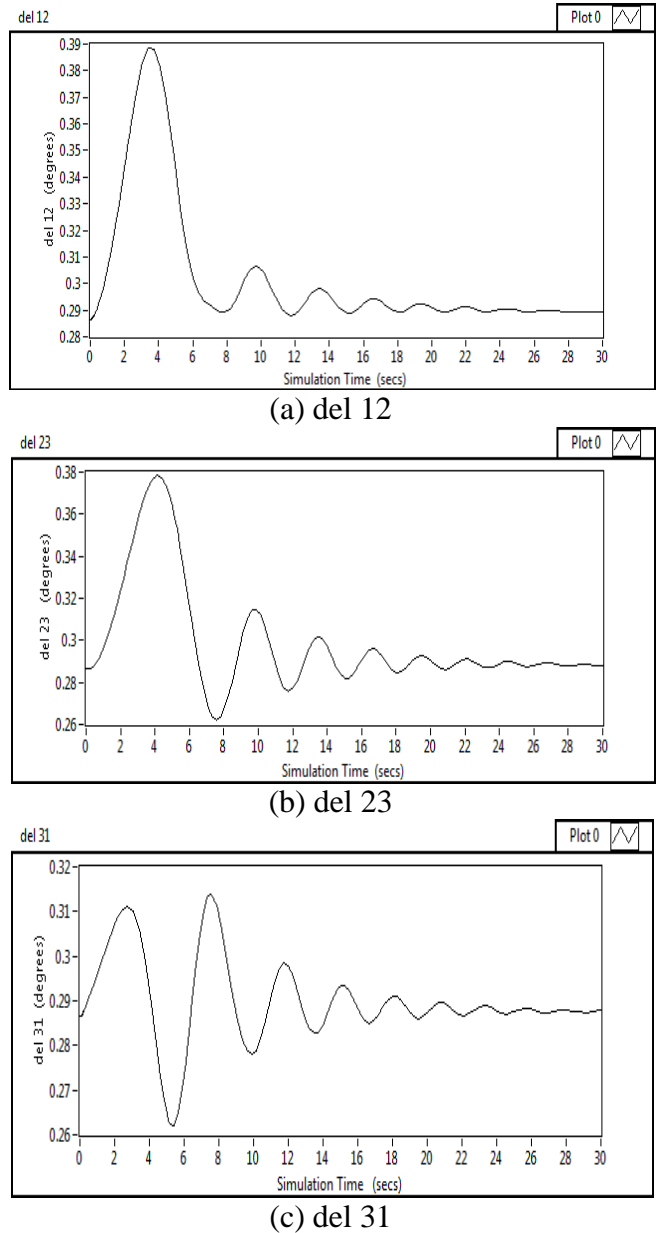
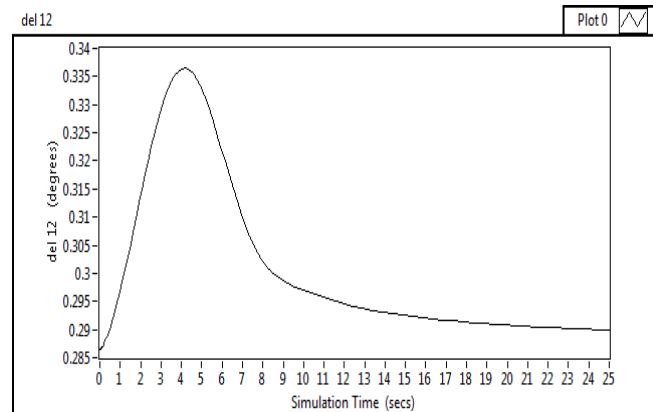
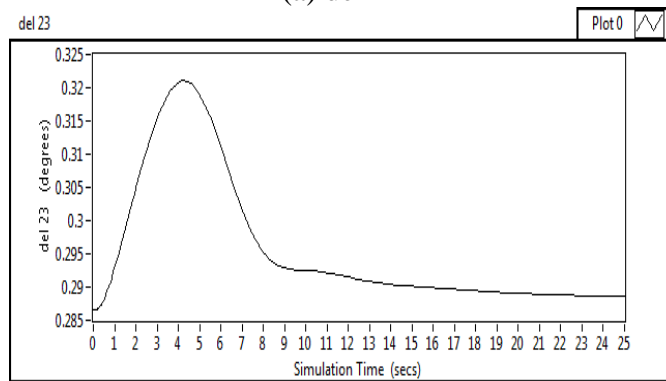


Figure 10: Variation of Relative Angular positions (del 12, del 23 and del 31) with time for $D_1 = D_2 = D_3 = 10$.

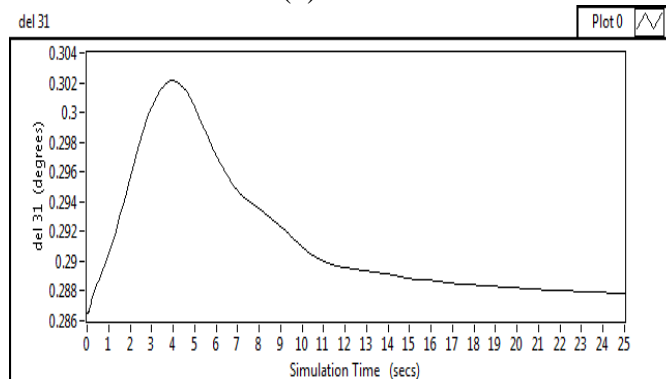
The final value of time taken to attain stability ie. 10-11 seconds does not further reduce even if the damping constants are further increased. This value is attained when $D_1 = D_2 = D_3 = 40$. If the value of damping constants are increased further, the maximum overshoot decreases and the system tends to behave as an over-damped sluggish system. This is clear from Fig.11 which shows the variation of relative angular positions (del 12, del 23 and del 31) with time, for $D_1 = D_2 = D_3 = 50$.



(a) del 12



(b) del 23



(c) del 31

Figure 11: Variation of Relative Angular Positions ($\text{del } 12$, $\text{del } 23$ and $\text{del } 31$) with time for $D_1 = D_2 = D_3 = 50$.

Keeping damping constants $D_1 = D_2 = D_3$ for varying values ranging from 5 to 50, the stable values, the time taken to attain stability, and the maximum overshoots of relative angular positions ($\text{del } 12$, $\text{del } 23$ and $\text{del } 31$) with time have been tabulated in Table III. It is observed from Table III that when the values of damping constants D_1 , D_2 , and D_3 are increased, the system becomes less oscillatory in nature. The time taken to attain stability by the system, decreases from the range of 57-58 seconds to

the range of 10-11 seconds. The maximum overshoot of the first swing also reduces from 0.42 to 0.32. It is also observed that the stable values of relative angular positions remained almost same at 0.287-0.29 degrees.

Table III: The Stable Values, The Time Taken to Attain Stability and The Maximum Overshoot of Relative Angular Positions (δ_{12} , δ_{23} and δ_{31}) with varying values of damping constant keeping $D_1 = D_2 = D_3$.

Damping Constant ($D_2=D_3$)	Damping Constant (D_1)	Stable Value of Relative Angular Positions (degrees)			Time Taken to Attain Stability (seconds)			Maximum Overshoot (degrees)		
		δ_{12}	δ_{23}	δ_{31}	δ_{12}	δ_{23}	δ_{31}	δ_{12}	δ_{23}	δ_{31}
5	5	0.2882	0.2867	0.288	53-54	47-48	57-58	0.42	0.39	0.35
10	10	0.2882	0.2876	0.2872	37-38	34-35	35-3	0.42	0.39	0.35
20	20	0.2893	0.2881	0.2876	18-19	21-22	20-21	0.42	0.39	0.35
30	30	0.2893	0.2882	0.2876	13-14	12-13	14-15	0.354	0.337	0.304
40	40	0.2893	0.2882	0.2876	10-11	11-12	13-14	0.345	0.327	0.303
50	50	0.2907	0.289	0.2882	10-11	11-12	10-11	0.336	0.32	0.302

Conclusion

The present LabVIEW based simulation has been successfully incorporated in the laboratory. The analysis of the simulation results revealed the following observations:

1. Simulation of SVC in LabVIEW helped to study the system behaviour, thus reducing its complexity. This is an easy-to-implement solution for a highly dynamic power system. This serves as a powerful graphical user interface, very near to the physical simulation. The implementation time is reduced and is open to further improvements and developments.
2. Simulation of various other FACTS controllers such as TCSC, STATCOM, UPFC and their different combinations can also be carried out using LabVIEW. This can act as a valuable tool for carrying out the transient stability analysis in depth. It promises a wide scope in enhancing transient stability limit, by providing better location of SVC and also by bringing in the cost-effectiveness for the power system.
3. SVC controller injects voltage into the line that changes the reactive power which in turn changes the rotor-angle and brings back the system into stable condition.
4. Stability of the system depends on the value of susceptance of the SVC controller which changes the value of the rotor-angle.
5. Upon reducing the values of damping constants D_1 , D_2 , and D_3 and keeping T_R and K_R as constants, it is observed that the time taken for the system to achieve stability increases significantly. This is due to the fact that by increasing the value of damping constants, the system's oscillations are reduced which helps the rotor-angle to attain a constant value at the point of stability.

References

- [1] S. Abazari, J. Mahdavi, M. Ehsan, and M. Zolghadri, "Transient Stability Improvement by Using Advanced Static Var Compensator", IEEE Bologna PowerTech Conference, June 23-26, Bologna, Italy, pp 1-7, 2003.
- [2] N. G. Hingorani, and L. Gyugyi, "Understanding FACTS concepts and Technology of Flexible AC Transmission Systems", IEEE Press, New York, 2000.
- [3] S. Chatterji, C. S. Rao, and T. K. Nagasarkar, "Fuzzy Logic based Half Wave Thyristor Controlled Dynamic Brake", 5th International Conference on Power Electronics and Drive Systems organized by IEEE in Singapore , 17-20 Nov.2003.
- [4] R. M. Mathur, R. K. Verma, "Thyristor based FACTS Controllers for Electrical Transmission Systems", IEEE Press, Piscataway 2002.
- [5] Y. Hongxiang, L. Mim, and J. Yanchao, "A Novel Topology of PWM Static VAR Compensator Based on the Concept of DC Fly back Converter", IEEE, 2004, pp. 769-775.
- [6] S. Panda, and N. Padhy, "Power System with PSS and FACTS Controller: Modelling, Simulation and Simultaneous Tuning Employing Genetic Algorithm", International Journal of Electrical, Computer and Systems Engineering, Vol.1, pp 9-18, 2007.
- [7] T. R. Jyothsna, and K. Vaisakh, "Improving Multi-Machine Transient Stability Using a Non- Linear Power System Stabilizer under Different Operating Conditions", Fifteenth National Power Systems Conference (NPSC), December, 2008.
- [8] R. Patel, V. Mahajan, and V. Pant, "Modelling of TCSC Controller for Transient Stability Enhancement", International Journal of Emerging Electric power Systems, Vol. 7, Issue 1, Article 6, pp 1-17, 2006.
- [9] R. Patel, T. S. Bhatti, and D. P. Kothari, "MATLAB/ Simulink based Transient Stability Analysis of a Multi-Machine Power System", International Journal of Electrical Engineering Education, Vol. 39, Issue 4, pp 320-336, October, 2002.
- [10] P. M. Anderson, and A. A. Fouad, "Power System Control and Stability", Science Press, Ephrata, Pa 17522, 1977.
- [11] R. H. Bishop, "Learning with LabVIEW 7TM Express", Pearson Education Publications, 2004.
- [12] R. Jayabarathi, M. R. Sindhu, N. Devarajan, and T. N. P. Nambiar, "Development of a Laboratory Model of Hybrid Static Var Compensator", IEEE Power India Conference, 10-12 April, pp 1-5, 2006.
- [13] T. Masood, A. A. Edris, and R. K. Aggarwal, "Static Var Compensator (SVC) modeling and analysis Techniques by MATLAB", PSC 2006, 13-15 Nov., Tehran-Iran, pp 1-7, 2006.